

# A plasmonic sensor design based on nanodots embedded metal-insulator-metal semi-ring resonator cavity

M.A. Butt<sup>1</sup>, S.A. Fomchenkov<sup>1,2</sup>, H.H. Mai<sup>3</sup>

<sup>1</sup>Samara National Research University, Moskovskoe Shosse 34A, Samara, Russia, 443086

<sup>2</sup>Image Processing Systems Institute of RAS - Branch of the FSRC "Crystallography and Photonics" RAS, Molodogvardejskaya street 151, Samara, Russia, 443001

<sup>3</sup>VNU University of Science, Vietnam National University, 334 Nguyen Trai, Hanoi, Vietnam

**Abstract.** In this work, we proposed a numerical study of a novel design of a highly sensitive plasmonic sensor based on a semi-ring cavity. The spectral characteristics and electric field distribution are studied using the finite element method. The standard sensor design shows a sensitivity of 600 nm/RIU which can be further enhanced by decorating nanodots in the cavity. The radius of nanodots plays a vital role in the amplification of SPPs in the cavity. It is shown that the total electric energy in the cavity enhances with the increase in the radius of the nanodots. Therefore, the nanodots decorated semi-ring cavity design can offer sensitivity and figure of merit of 1084.21 nm/RIU and 57.06, respectively.

## 1. Introduction

Surface plasmon polaritons (SPPs) are optical waves, emerging from incident photons coupled with free electrons on the metal surface [1]. The E-field intensity of SPPs is strongly bound along with the metal-dielectric interface and decays drastically in the direction vertical to the interface [2]. The MIM WG is most extensively used plasmonic-based nanostructures for the realisation of integrated optical circuits. MIM WGs are plasmonic structures in which an insulator is enclosed by two metal claddings. The straightforward design and capability of these WGs to confine light at the subwavelength level are the key features of this system. To realise highly integrated optical circuits, researchers have conducted rigorous research on the design of various devices using MIM WGs. These devices include filters [3], sensors [4], switches [5], couplers [6], splitters [7], among others. Refractive index sensors have many uses in the biological and chemical fields and have been intensively researched in recent years, such as the concentration of the solution and pH value, that can be calculated by changes in refractive index. When a substance under investigation is brought into contact with the sensor,  $n_{eff}$  of the MIM WG changes, and as a result, the redshift of the  $\lambda_{res}$  is observed. SPs are very sensitive to changes in the refractive index in the proximity of the surface.

## 2. Device design

In this paper, a simple and novel plasmonic sensor design is presented, which consists of a semi-ring cavity side coupled to a MIM bus WG. The geometric parameters of the sensor design are  $L$ ,  $w$ ,  $r_s$ ,  $r$  and  $d$  which represents the length of the bus WG, the width of bus WG, the width of the semi-ring cavity, radius of the semi-ring and distance between bus WG and the semi-ring, respectively. For NDs decorated design, NDs are represented by  $ND_r$ . The geometric parameters of the designs are presented in table 1. A finite element method (FEM) is used to simulate the transmission spectrum and

E-field distributions using commercially available COMSOL software. The schematic representation of standard MIM semi-ring resonator and *NDs* decorated MIM semi-ring resonator is shown in figure 1.

**Table 1.** The geometric parameters of the sensor design.

$L$ (nm)	$w$ (nm)	$d$ (nm)	$rI$ (nm)	$r$ (nm)	$ND\_r$ (nm)
1500	50	50	50	300	5, 10, 15, 20, 24

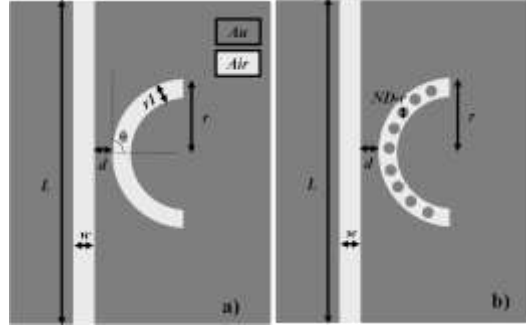


**Figure 1.** Schematic of a) MIM semi-ring resonator, b) *NDs* decorated MIM semi-ring resonator.

The metal and insulator materials are defined as gold (*Au*) and air, respectively. *Au* is desired as the metal layer due to its biocompatibility and resistance to oxidation compared to silver (*Ag*). The refractive index of *Au* is calculated from the Drude model:  $\varepsilon = \varepsilon_{\infty} - \frac{\omega_p^2}{\omega^2 + j\omega\gamma}$ , Where  $\varepsilon_{\infty} = 9.0685$ ,  $\omega_p = 135.44 \times 10^{14}$  rad/s and  $\gamma = 1.15 \times 10^{14}$  rad/s [8]. The TM mode of the MIM bus WG is excited by a plane wave. As  $w \ll \lambda_{\text{incident}}$ , so only fundamental TM mode can exist. The dispersion relation of this fundamental mode is described as:

$$\frac{\varepsilon_i p}{\varepsilon_m k} = \frac{1 - e^{kw}}{1 + e^{kw}}$$

$$k = k_o \sqrt{\left(\frac{\beta_{spp}}{k_o}\right)^2 - \varepsilon_i p} = k_o \sqrt{\left(\frac{\beta_{spp}}{k_o}\right)^2 - \varepsilon_m}$$

$$\beta_{spp} = n_{eff} k_o = n_{eff} \frac{2\pi}{\lambda}$$

Here  $w$  refers to the width of the bus WG,  $\lambda$  shows incident light wavelength in vacuum,  $\varepsilon_i$  and  $\varepsilon_m$  give the relative dielectric and metal permittivity,  $\beta_{spp}$  and  $n_{eff}$  are propagation constant and effective refractive index of SPPs, and  $k_o = 2\pi/\lambda$  is the wavenumber.

### 3. Sensing performance

In general, ring resonators are susceptible to ambient refractive index and their  $\lambda_{res}$  displays redshift with increasing refractive index. Here, two significant factors such as sensitivity ( $S$ ) and the figure of merits ( $FOM$ ) are discussed which is used to evaluate the sensing performance of sensors. The device  $S$  is defined as the ratio of the change in  $\lambda_{res}$  to the change of the ambient refractive index i.e.  $S = \lambda_{res}/\Delta n$ . The potential to evaluate small changes in the refractive index of a plasmonic sensor is directly proportional to  $S$  and is also inversely proportional to resonance width (spectral dip or peak). The combinations of these parameters are often referred to as the figure of merits and are described as  $FOM = S/FWHM$ . The spectral response of the sensor is calculated by filling the medium with several refractive indices. The normalized intensity at the output bus WG is calculated in visible and NIR wavelength range at  $n=1.0-1.38$ . Here,  $S$  is calculated for standard and *NDs* decorated MIM semi-ring cavity resonator as shown in figure 2. The positive impact of  $ND\_r$  on  $S$  can be observed. As a result,  $S_{max}$  is obtained at 1084.21 nm/RIU for  $ND\_r = 24$  nm. The  $FOM$  of the *NDs* decorated MIM semi-ring cavity resonator is approximately 57.06.

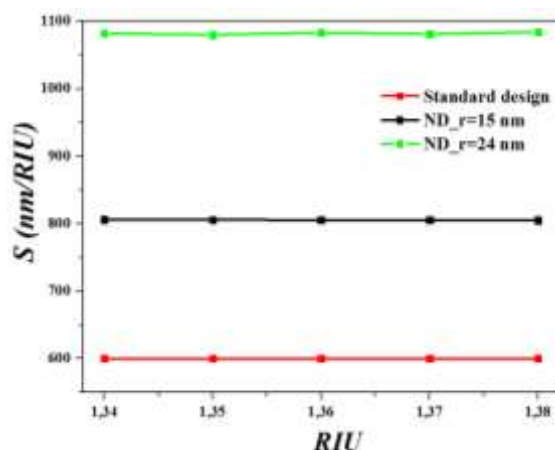


**Figure 2.** The sensitivity of standard and *ND* decorated MIM semi-ring cavity resonator.

#### 4. Conclusion

We suggested a numerical study of a novel design of a highly sensitive plasmonic sensor based on a semi-ring cavity resonator. The standard sensor design shows a reasonable sensitivity of 600 nm/RIU which can be further enhanced by decorating nanodots in the cavity. The radius of nanodots has a critical role in the amplification of SPPs in the cavity. The total electric energy in the cavity enhances with the increase in the radius of the nanodots. Therefore, the nanodots decorated semi-ring cavity design can offer sensitivity and *FOM* of 1084.21 nm/RIU and 57.06, respectively. The proposed sensor design shows great potential for nanophotonic applications.

#### 5. Acknowledgements

This research was supported by the International Centre for Genetic Engineering and Biotechnology (ICGEB) through a grant to Dr. Hanh Hong Mai. Grant no. CRP/VNM17-03. Also, this work was supported by RFBR grant # 18-58-14001.

#### 6. References

- [1] Barnes, W.L. Surface plasmon subwavelength optics / W.L. Barnes, A. Dereux, T.W. Ebbesen // *Nature*. – 2003. – Vol. 424. – P. 824-830.
- [2] Zhang, J. Surface plasmon polaritons: Physics and Applications/ J. Zhang, L. Zhang, W. Xu // *Journal of Physics D: Applied Physics*. – 2012. – Vol. 45(11). – P. 113001.
- [3] Wang, L. A triangular-shaped channel MIM waveguide filter / L. Wang, L. Wang, Y.-P. Zeng, D. Xiang, Z. Xiang, X.-F. Li // *Journal of Modern Optics*. – 2012. – Vol. 59(19). – P. 1686-1689.
- [4] Butt, M.A. An array of nano-dots loaded MIM square ring resonator with enhanced sensitivity at NIR wavelength range / M.A. Butt, S.N. Khonina, N.L. Kazanskiy // *Optik*. – 2020. – Vol. 202. – P. 163655.
- [5] Yi, X. Transmission characteristics of a Y-shaped MIM plasmonic waveguide with side-coupled cavities / X. Yi, J. Tian, R. Yang // *Opto-Electronic Engineering*. – 2017. – Vol. 44. – P. 1004-1013.
- [6] Kong, D. Evaluation of slot-to-slot coupling between dielectric slot waveguides and metal-insulator-metal slot waveguides / D. Kong, M. Tsubokawa // *Optics Express*. – 2015. – Vol. 23. – P. 19082-19091.
- [7] Xiang, D. MIM plasmonic waveguide splitter with tooth-shaped structures / D. Xiang, W. Li // *Journal of Modern Optics*. – 2014. – Vol. 61. – P. 222-226.
- [8] Sia, P.D. Overview of Drude-Lorentz type models and their applications // *Nanoscale Syst.: Math. Model. Theory Appl.* – 2014. – Vol. 3. – P. 1-13.